

Effects of Co ratio on fatigue life of WC-Co die inserts used in cold forming operations

HIZLI Burak^{1,2,a*}, OZTURK Kubra^{1,2,b}, INCE Umut^{2,c}

¹Department of Metallurgical and Materials Engineering, Dokuz Eylul University, İzmir, Türkiye

²R&D Center, Norm İzmir Cıvata San. ve Tic. A.Ş., AOSB, İzmir, Türkiye

^aburak.hizli@normfasteners.com, ^bkubra.ozturk@normfasteners.com,
^cumut.ince@normfasteners.com

Keywords: WC-Co, Co Ratio, Fatigue Life, Cold Forming

Abstract. Production of fasteners via cold forming requires high forming forces, which induce significant stresses in dies. Therefore, die performance becomes a critical parameter of the fastener production process. Estimation of die life with high accuracy allows to enhance production efficiency and reduce die-related expenditures. Generally, WC-Co hardmetals consisting of 4-30% Co content as a binder are highly preferred in cold forming operations. WC-Co metal-ceramic composite materials offer high wear resistance against frictional forces, high compressive strength, and lower elastic deformation to resist excessive contact pressures, which are primary requirements for cold-forming dies. In this study, experimental investigations were conducted for the determination and comparison of fatigue performance at three different stress amplitudes, utilizing three-point bending fatigue testing with two different grades of WC-Co hardmetals. After the experiments, Goodman-Haigh diagrams were obtained from the experimental results to be utilized in predictive die-life calculations.

Introduction

Tungsten carbide-cobalt materials are ceramic-matrix composite materials with high wear resistance, consisting of a WC as a hard phase and Co as a soft binding phase. Low cobalt content in a hardmetal causes large gaps between WC grains, resulting in a material with lower toughness and resistance to fatigue [1]. Various combinations are formed depending on the content of the Co binder, and they are used in different industries according to the needs, ranging from automotive parts production to the mining sector [1, 2]. Die materials used in the cold forming process require high fracture toughness to prevent crack propagation, wear resistance, and high fatigue strength due to the high forming forces that create significant stresses in the dies. [2]. As a consequence, die life has a direct and significant impact on several factors, including mass production, production plans, costs, and customer satisfaction. In the studies conducted in the literature on this subject, Tanrikulu et al. examined three-point bending fatigue tests on specimens of WC-20 wt.% Co, which are often used in cold forging dies, with a loading ratio (R) of 0.1, and constructed Morrow-Haigh diagrams to determine the fatigue life. Through comparison of three-point bending test results with production line dies, their model accurately predicted fatigue life with a deviation of only 5.6 % [3]. The research conducted by Klünser et al. investigated various grades with variations in WC grain size and Co binder content, ranging from 0.2 to 1.3 μm and 6 to 12 wt.%, respectively. They demonstrated that the fatigue crack growth behavior of a hardmetal alloy with an ultra-fine WC grain size showed a dependency on the stress ratio. The threshold stress intensity factor range for fatigue crack growth from inhomogeneities was found to vary with stress ratios, with values of 4.3, 6.2, and 9 MPa for R=0.1, -1, and -3, respectively [4]. Ferreira et al. examined the mechanical behavior of WC-Co materials with different Co ratios (R=0.05 and R=0.5) and demonstrated the influence of Co content on ductility and brittleness [5]. Mikado et al. investigated

the fatigue strength of WC-Co materials using a three-point bending test with $R=0.5$ and analyzed S-N diagrams [6]. A study by Torres et al. aimed to assess the fatigue behavior of a fine-grained WC-10 wt.% Co hardmetal. It specifically examined the influence of mean stress on the fatigue limit of hardmetals, suggesting that this influence could be elucidated through a Goodman-like relationship [7]. Li et al. examined the fatigue strengths of WC-Co samples with Co binder contents ranging from 3 to 20 wt. % were compared based on their Co content. Having an in-depth knowledge of the mechanical properties of WC-Co will enable companies to determine the most suitable composite structure for various types of industrial processes [8]. Therefore, the fatigue performance of two different grades of WC-Co hardmetals was meticulously investigated and compared in this study. Experimental investigations were conducted for the determination and comparison of fatigue performances at three different stress amplitudes, utilizing three-point bending fatigue testing with two different grades of WC-Co hardmetals. After the completion of experiments, Goodman-Haigh diagrams were obtained from the experimental results.

Materials & Methods

In this study, different grades of WC-Co materials that have Co contents of 19 and 26% were used in the experiments in order to reveal the fatigue life performance of die inserts used in heading and upsetting operations. Referenced grades were supplied from Boehlerit GmbH & Co.KG with corresponding product range numbers of GB40 and GB56, respectively. The chemical compositions, and mechanical and physical properties of these grades shared by the supplier are given in Table 1. All the test samples were produced by sintering WC powder with Co binder using special molds and HIPed to fabricate the test samples without machining.

Table 1. Properties of referenced grades.

Grade	Chemical Composition [wt. %]			Density [g/cm ³]	Hardness HV 30 [MPa]	Compressive Strength [MPa]	Transverse Rupture Strength [MPa]	Fracture Toughness [MNm ^{-3/2}]	Elastic Modulus [GPa]	Thermal Expansion Coefficient [10 ⁻⁶ / K]
	WC	Co	Other							
GB40	Balanced	19	<0.2	13.60	950	4,000	2800	≥ 24	530	6
GB56	Balanced	26	<0.2	13.05	815	3,200	2700	≥ 24	490	6.5

It is crucial to decrease the surface roughness of forming dies in order to prevent excessive frictional effects that could cause high forming forces and, in return, lower the die life during cold forming. Therefore, prior to testing stage, the surfaces of the test samples were grinded and polished to obtain surface conditions similar to forming dies. Surface preparations were completed in two steps: (i) grinding of each surface with 220+ grid diamond disc under 40 N for 3 min. at 400 rpm, and (ii) polishing of each surface with 9 – 3 μm diamond disc under 25 N for 5 min. at 400 rpm. Surface preparation steps were carried out using Metkon Forcipol 102 grinding and polishing machine with Metkon Forcimat 102 automatic head. Following the microstructural observations, the surface roughness of grinded and polished surfaces of samples was measured by Mitutoyo SurfTest SJ 210 portable surface roughness measurement instrument in terms of R_a , R_q , and R_z values. During the measurements, roughness values of the polished surfaces were measured with a straight line pattern over a sampling length of 4.8 mm, in accordance with ISO 1997. Additionally, microstructural observations were conducted on samples of both grades using Zeiss Axio Imager.M2m optical microscope on the polished surfaces.

Fatigue life tests were carried out on prismatic test samples using a three-point bending test apparatus adapted to Zwick Roell Amsler 250 FP 5100 high-frequency fatigue testing machine. Test samples were produced according to Type B as given in ISO 3327:2009, whose nominal dimensions are 20x6.5x5.25 mm [9]. Test samples and fatigue testing stage are illustrated in Fig.

1a and Fig. 1b, respectively. Stress amplitudes in fatigue tests were determined as 750, 800, and 850 MPa in order to observe the fatigue behavior in a wide range of loading conditions. Stress ratios (R) were determined using minimum stress (σ_{min}) and maximum stress (σ_{max}) values in a cycle as given in Eq. 1. Mean stresses (σ_m) and stress amplitudes (σ_a) were sequentially calculated by the formulas in Eq. 2 and Eq. 3 as given below.

$$R = \frac{\sigma_{min}}{\sigma_{max}} \tag{1}$$

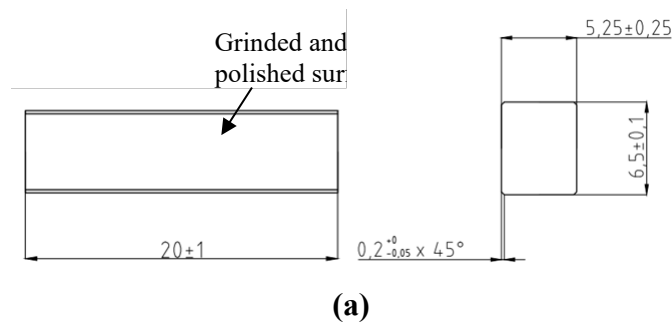
$$\sigma_m = \frac{\sigma_{max} + \sigma_{min}}{2} \tag{2}$$

$$\sigma_a = \frac{\sigma_{max} - \sigma_{min}}{2} \tag{3}$$

Maximum and minimum loads in fatigue tests were calculated for corresponding maximum and minimum stress values based on stress ratios of $R=0.1$ and $R=0.2$ by using Eq. 4 which is given in ISO 3327:2009 as;

$$R_{bm} = \frac{3kFl}{2bh^2} \tag{4}$$

where R_{bm} is transverse rupture strength in MPa, F is the force applied to the test piece in N, k is the correction factor to compensate for the chamfer, l is the distance between supports, b is the width of test piece perpendicular to its height, and h is the height of test piece parallel to the direction of application of the test force, respectively. k value was taken as 1, as described in the standard for test samples having chamfer of 0,15 to 0,2 mm.



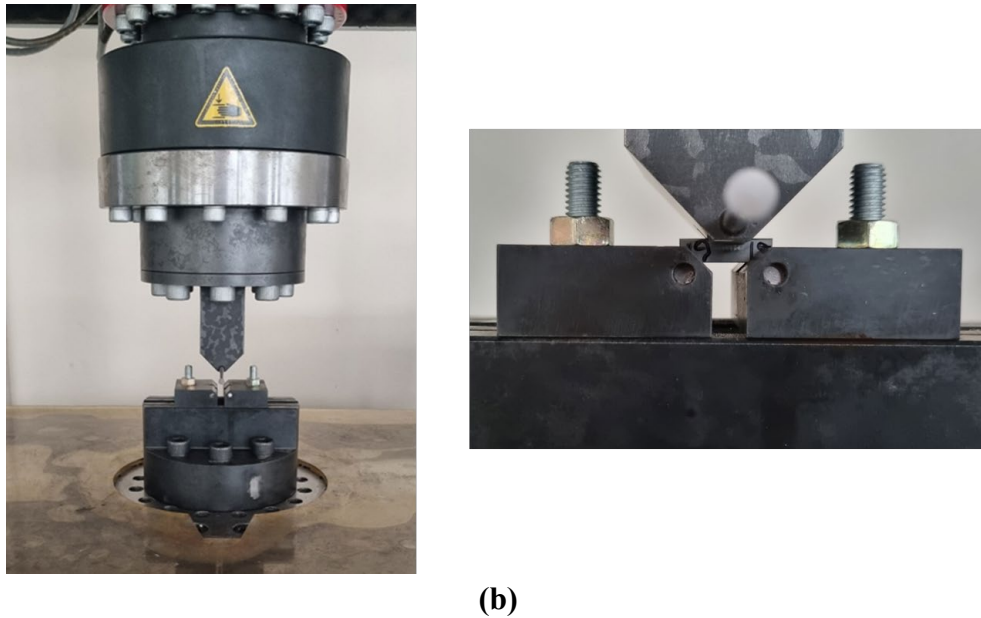


Fig. 1. (a) Dimensions of prismatic samples used in the testing stage and (b) testing fixtures used in fatigue tests and sample positioning.

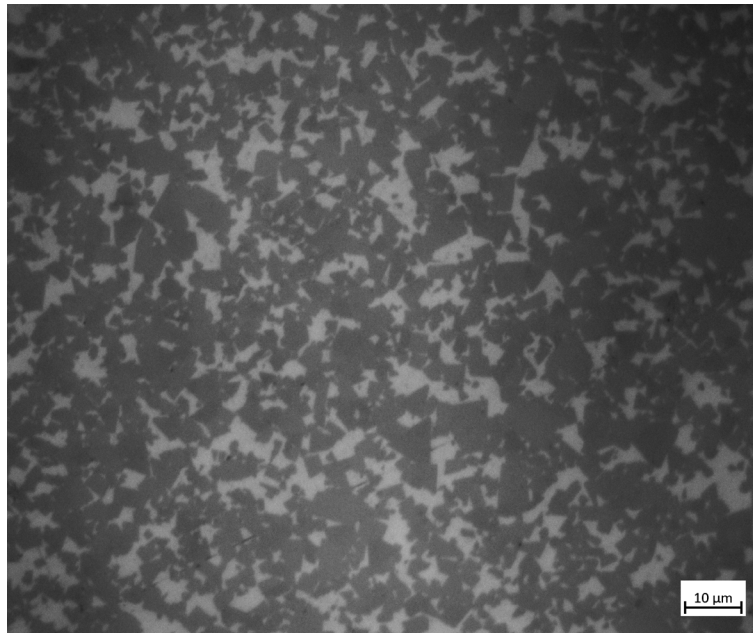
Calculated static and dynamic forces in fatigue tests corresponding to maximum, minimum, and mean stress values are given in Table 2. The endurance limit for fatigue tests was accepted as 5,000,000 cycles. The average fatigue performance of each set was determined from consistent 3 test results. S-N curves and Goodman-Haigh diagrams were obtained and compared from test results of each grade in order to correlate test results with life cycles of forming dies during the cold forming operations.

Table 2. Fatigue test parameters and corresponding static and dynamic loads.

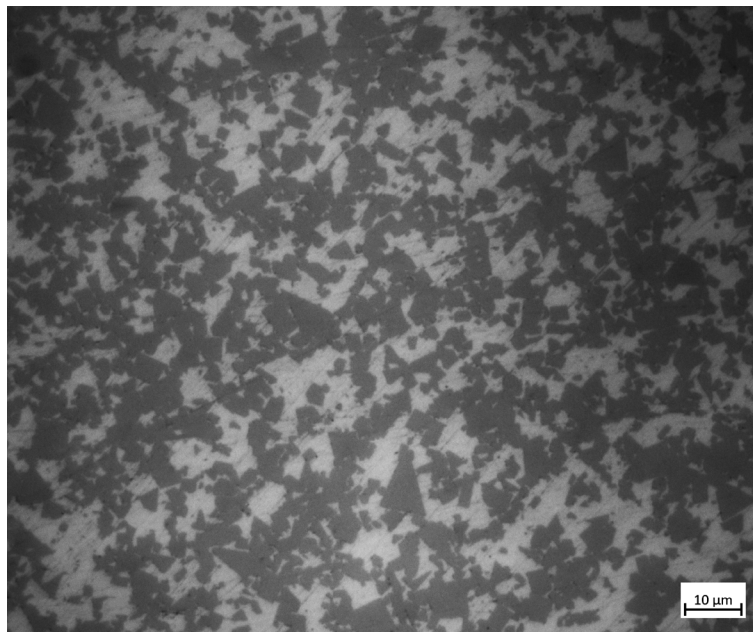
Stress Ratio [R]	Stress Amplitude, σ_a [MPa]	Min. Stress, σ_{min} [MPa]	Max. Stress, σ_{max} [MPa]	Mean Stress, σ_m [MPa]	Static Load [kN]	Dynamic Load [kN]
0.1	850	188.9	1,888.9	1,038.9	6.20	5.08
	800	177.8	1,777.8	977.8	5.84	4.78
	750	166.7	1,666.7	916.7	5.47	4.48
0.2	850	425	2,125	1,275	7.61	5.08
	800	400	2,000	1,200	7.17	4.78
	750	375	1,875	1,125	6.72	4.48

Results & Discussions

OM micrographs of both grades are shown in Fig 2a and 2b, respectively. WC powders in Co binder exhibited homogenous distributions regardless of the amount of Co binder. However, the difference in the amount of Co binder depending on grade was identified from the micrographs. WC powders with an average particle size of 6.6 μm were used during the fabrication of GB40 samples. For GB56 samples, the average particle size of WC particles was found as 6.1 μm .



(a)



(b)

Fig. 2. OM micrographs of (a) GB40 and (b) GB56.

Surface roughness results obtained from grinded and polished samples are given in Table 3. According to the results, it was seen that values exhibited convergent and even superior values compared to those of forming dies. Also, surface roughness results were in well-conforming manner to surface conditions outlined in ISO 3327:2009, which is defined as not exceeding R_a limit of $0,4 \mu\text{m}$. These findings are evident that failure in fatigue tests is expected to originate from inner defects rather than surface conditions.

Table 3. R_a , R_q , and R_z values of test samples.

Grade	R_a (μm)	R_q (μm)	R_z (μm)
GB40	0.036 ± 0.010	0.044 ± 0.05	0.255 ± 0.031
GB56	0.046 ± 0.021	0.058 ± 0.026	0.275 ± 0.098

Three-point bending fatigue test results of GB40 and GB56 insert materials are listed in Tables 4 and 5 in detail, respectively. For both grades, fatigue test results showed a consistent manner with each other considering stress ratio, stress amplitude, and hardness increase with Co content decrease.

Table 4. Fatigue test results of GB40 samples.

Stress Ratio [R]	Static Load [kN]	Dynamic Load [kN]	Stress Amplitude [MPa]	Cycles to Failure	Average Cycles to Failure	
0.1	6.20	5.08	850	268,396	$438,316 \pm 221,767$	
	6.20	5.08	850	357,366		
	6.20	5.08	850	689,185		
	0.1	5.84	4.78	800	772,647	$2,144,884 \pm 2,473,221$
		5.84	4.78	800	662,006	
		5.84	4.78	800	5,000,000	
		5.47	4.48	750	5,000,000	
		5.47	4.48	750	5,000,000	
	0.2	7.61	5.08	850	179,076	$174,419 \pm 74,119$
7.61		5.08	850	98,081		
7.61		5.08	850	246,101		
0.2		7.17	4.78	800	431,630	$310,732 \pm 136,040$
		7.17	4.78	800	163,423	
		7.17	4.78	800	337,144	
		6.72	4.48	750	463,139	
		6.72	4.48	750	811,459	
0.2		6.72	4.48	750	827,372	$700.656 \pm 205,850$

Table 5. Fatigue test results of GB56 samples.

Stress Ratio [R]	Static Load [kN]	Dynamic Load [kN]	Stress Amplitude [MPa]	Cycles to Failure	Average Cycles to Failure
0.1	6.20	5.08	850	114,737	$87,383 \pm 36,755$
	6.20	5.08	850	45,603	
	6.20	5.08	850	101,808	
0.1	5.84	4.78	800	208,056	

	5.84	4.78	800	65,142	127,365 ±
	5.84	4.78	800	108,896	73,225
	5.47	4.48	750	97,394	269,746 ± 205,725
	5.47	4.48	750	497,502	
	5.47	4.48	750	214,342	
0.2	7.61	5.08	850	22,276	25,083 ± 8,244
	7.61	5.08	850	34,365	
	7.61	5.08	850	18,609	
	7.17	4.78	800	100,492	74,994 ± 22,536
	7.17	4.78	800	66,745	
	7.17	4.78	800	57,744	
	6.72	4.48	750	122,389	123,889 ± 53,824
	6.72	4.48	750	70,831	
	6.72	4.48	750	178,448	

According to fatigue test parameters given in Table 2, maximum, minimum and mean stress levels considerably altered as the stress ratio increased to $R=0.2$. Because of this reason, cycles to failure in $R=0.2$ were significantly decreased compared to cycles acquired from $R=0.1$ tests. It is generally anticipated that WC-Co grades with higher binder content exhibit greater toughness than grades with lower binder content, resulting in improved performance in resisting higher forming loads during cold forming operations. Consequently, WC-Co grades with higher binder content demonstrate increased resistance to cyclic loads, as evidenced by an extended cycle-to-failure capability. Additionally, lower binder content leads to increased brittleness, so toughness decreases. However, in contrast to having a lower binder content than the other grade, the results of GB40 grade were well above those obtained from GB56 grade, considering both stress ratios and each stress amplitude. Despite GB56 tests, several tests on GB40 grade which were conducted at various stress amplitudes and stress ratios resulted in run-out and reaching the endurance limit. These results were attributed to the probability of the existence of $<0.2\%$ other elements such as Cr and Mo in GB40 grade that improve the material properties. As comparing the two referenced grades, GB40 results exhibited noticeable scattering in all test sets, even higher in test sets of low mean stress-stress amplitudes. It is noteworthy to be said that inner defects and their severeness become critical influencing criteria in terms of fatigue performance and eventual cycles to failure. For any stress combinations lying within the limit areas of $R=0.2$ with stress amplitude of 750 MPa and $R=0.1$ with stress amplitude of 800 MPa evidently showed the effect of the previous statement. Additionally, having slightly bigger sized WC powders by GB40 was predicated as an accompanied factor to result in better fatigue performance than GB56 due to lowering crack propagation rates. These outcomes would be further investigated and verified through elemental analysis and examination of fracture surfaces. Also, test results would be confirmed in real-world applications for usage in die life simulations and production trials of die inserts built by using GB40 and GB56 grades.

Following the testing stage, obtained test results were employed to draw Goodman-Haigh diagrams that would be utilized in die life estimations of WC-Co die inserts. Respective diagrams for both GB40 and GB56 grades are illustrated in Fig. 3 and Fig. 4. With the help of these diagrams, die lifes and safe stress limits could be estimated based on determined areas separated by fitted lines of cycle-to-failure limits, also identifying the corresponding mean stress-stress amplitude ranges in which the die insert could perform reliably.

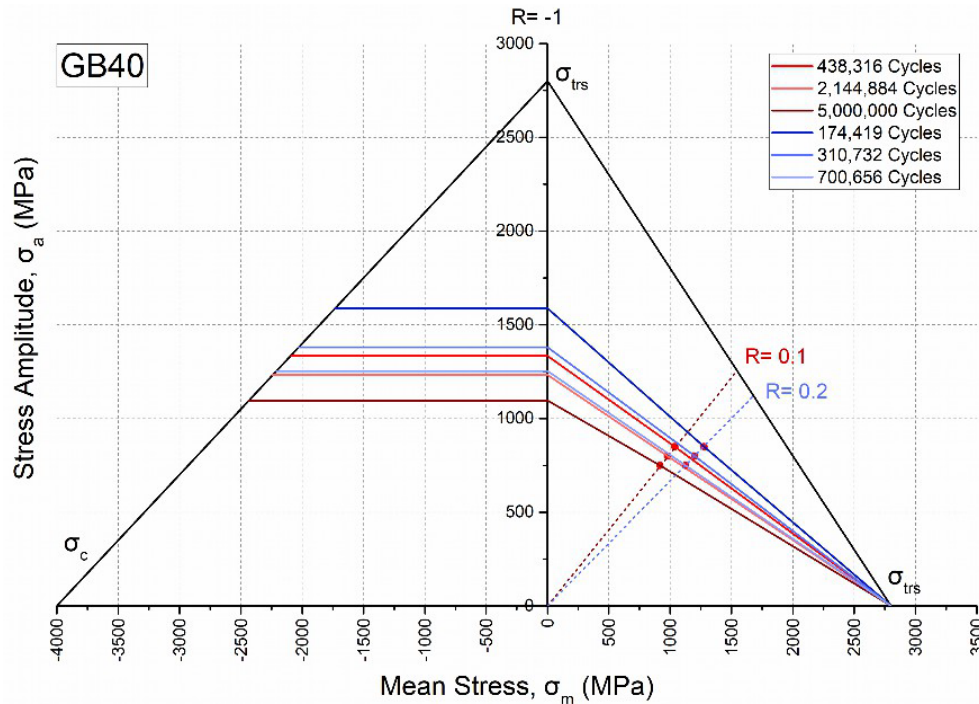


Fig. 3. Goodman-Haigh diagram of GB40 grade for $R=0.1$ and $R=0.2$.

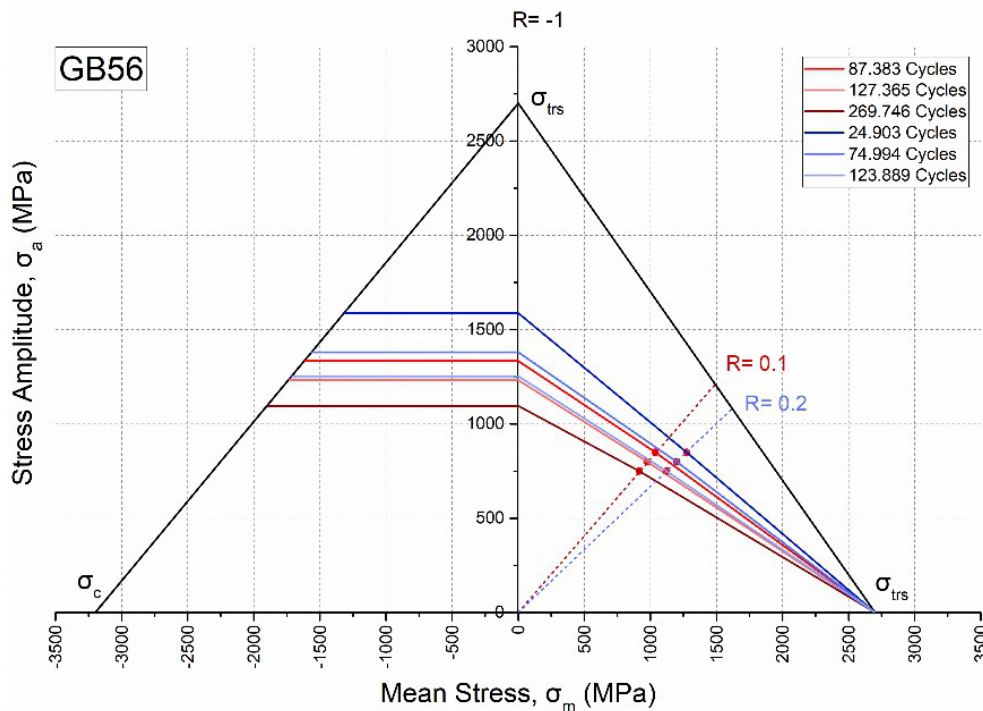


Fig. 4. Goodman-Haigh diagram of GB56 grade for $R=0.1$ and $R=0.2$.

As the fatigue tests at $R=-1$ stress ratio could not be conducted for the three-point bend samples of hardmetals, the transverse rupture strength of such hardmetals was utilized as static failure strength instead of the ultimate tensile strength value in the Goodman-Haigh graph. In contrast to diagrams that are drawn for materials with infinite fatigue life, diagrams for hardmetals help to define stress limits and corresponding fatigue life limits. Therefore, fitted lines based on mean

stress-stress amplitude values illustrate the most probable cycles until failure due to fatigue and life zones placed on each fitted line are restricted with other lines that show a lower fatigue life. The Goodman-Haigh diagrams were extended to include the compression zone, facilitating the adjustment of the acquired lines to the compression characteristics of the material. With the utilization of the shrink-fitting process in cold forming dies, there is a need for a comprehensive fatigue life map that takes into account the compressive stresses present in the core material of WC-Co die inserts due to shrink-fitting. The compressive strength of the material represents the static failure strength on the compression zone of the diagram, which was taken as 4,000 MPa and 3,200 MPa for GB40 and GB56, respectively. The diagrams given in Fig. 3 and Fig. 4 would directly be used to predict the most probable fatigue lives of GB40 and GB56 in the case of being exposed to several mean stress and stress amplitude combinations. Additionally, fatigue life limits for the $R=-1$ stress ratio could be determined from where the fitted limit lines meet the stress amplitude axis and then S-N diagrams would be drawn for each stress amplitude accordingly. Though the fatigue endurance limit of GB40 was found as 1096 MPa directly from diagrams for zero mean stress condition, the determination of the fatigue endurance limit of GB56 required further tests in lower mean stress-stress amplitude values rather than those reported above.

Conclusions

In the scope of this study, two different grades of WC-Co materials that sequentially have Co contents of 19 and 26% were tested and investigated to understand the effects of Co content on the fatigue life of WC-Co die inserts, which are highly preferred materials in heading and upsetting operations due to high resistance against frictional forces and high contact pressures, superior compressive strength, and lower elastic deformation under forming forces. The following conclusions can be extracted from the experimental results and Goodman-Haigh diagrams:

- Fatigue tests were conducted after reaching lower surface roughness values in order not to cause failure by the surface defects, originating from inner flaws and defects.
- GB40 (WC-19 wt.% Co) grade exhibited better fatigue performance compared to GB56 (WC-26 wt.% Co) in contrast to its increased sensitivity to brittleness due to less binder content and higher hardness.
- Superior test results obtained from GB40 grade were attributed to the probability of existence of <0.2 % other elements such as Cr and Mo. The addition of such elements in WC-Co grade is likely to improve the material properties including fatigue resistance.
- As the Co content decreased, the standard deviation for the same sets increased.
- Goodman-Haigh diagram of both GB40 and GB56 grades were drawn by utilizing experimental results. Die life estimations and determination of safe stress limits could be made based on determined areas separated by fitted lines of cycle-to-failure limits, also identifying the corresponding mean stress-stress amplitude ranges in which the die insert could perform reliably.
- Stress amplitude values read for $R=-1$ stress ratio conditions when the respective limit lines cross the vertical axis in Goodman-Haigh diagrams could be used to construct an S-N diagram of zero mean stress condition.

The aforementioned experimental outcomes would be further investigated and verified through elemental analysis, and examination of fracture surfaces. Fatigue test results are planned to be confirmed in real-world applications for usage in die life simulations and production trials of dies built by using GB40 and GB56 grade die inserts as a part of future investigations.

References

- [1] H.M. Ortner, P.Ettmayer, H. Kolaska, I.Smid, The history of the technological progress of hardmetals, *International Journal of Refractory Metals and Hard Materials*, 49 (2015) 3-8. <https://doi.org/10.1016/j.ijrmhm.2014.04.016>
- [2] J.García, V.C. Ciprés, A. Blomqvist, B. Kaplan, Cemented carbide microstructures: a review, *International Journal of Refractory Metals and Hard Materials*, 80 (2019) 40-68. <https://doi.org/10.1016/j.ijrmhm.2018.12.004>
- [3] B.Tanrikulu, R. Karakuzu, Fatigue life prediction model of WC-Co cold forging dies based on experimental and numerical studies, *Engineering Failure Analysis*, 118 (2020) <https://doi.org/10.1016/j.engfailanal.2020.104910>
- [4] T.Klünsner, S.Marsoner, R. Ebner, R. Pippan, J. Glätzle, A.Püschel, Effect of microstructure on fatigue properties of WC-Co hardmetals, *Procedia Engineering* 2 (2010) 2001-2010. <https://doi.org/10.1016/j.proeng.2010.03.215>
- [5] J.A.M. Ferreira, M.A. Pina Amaral, F.V. Antunes, J.D.M. Costa, A study on the mechanical behaviour of WC/Co hardmetals, *International Journal of Refractory Metals and Hard Materials* 27 (2009) 1-8. <https://doi.org/10.1016/j.ijrmhm.2008.01.013>
- [6] H. Mikado, S.Ishira, N. Oguma, K.Masuda, S. Kitawaga, S.Kawamura, Effect of stress ratio on fatigue lifetime and crack growth behavior of WC–Co cemented carbide, *Transactions of Nonferrous Metals Society of China* 24(2014) 14-19. [https://doi.org/10.1016/S1003-6326\(14\)63282-9](https://doi.org/10.1016/S1003-6326(14)63282-9)
- [7] Y.Torres, M. Anglada, L.Llanes. Fatigue mechanics of WC–Co cemented carbides, *International Journal of Refractory Metals and Hard Materials*, 19(2001) 341-348. [https://doi.org/10.1016/S0263-4368\(01\)00032-4](https://doi.org/10.1016/S0263-4368(01)00032-4)
- [8] A.Li, J.Zhao, D.Wang, X. Gao, H. Tang, Three-point bending fatigue behavior of WC–Co cemented carbides, *Materials & Design* 45(2013) 271-278. <https://doi.org/10.1016/j.matdes.2012.08.075>
- [9] *Hardmetals - Determination of transverse rupture strength*, ISO 3327:2009 (2009)